Optical properties of Er^{3+} doped alkali chlorophosphate glasses for optical amplifiers

K. Pradeesh [a], C.J. Oton [b], V.K. Agotiya [a], M. Raghavendra [a], G. Vijaya Prakash [a,*]

[a] *Nanophotonics Laboratory, Department of Physics, Indian Institute of Technology Delhi, New Delhi 110016, India*
[b] *Optoelectronics Research Centre, University of Southampton, Southampton SO17 1BJ, UK*

Abstract

A new class of Erbium doped glasses with compositions xNa$_2$O–(60 − x) PbCl$_2$–40P$_2$O$_5$ (x = 0, 10, 20 and 30) were fabricated and characterized for optical properties. Absorption spectra were analyzed for important Judd–Ofelt parameters from the integrated intensities of various Er^{3+} absorption bands. A systematic correlation between the Judd–Ofelt parameter Ω_2 and the covalent nature of the glass matrix was observed, due to the increased role of bridging oxygens in the glass network. Photoluminescence (PL) and its decay behavior studies were carried out for the transition $^4I_{13/2} \rightarrow ^4I_{15/2}$. The PL broadness and life times were typically in the range of 40–60 nm and 2.13–2.50 ms, respectively. These glasses show high transparency, high refractive index, shorter life times and, most importantly, these glasses were capable of being doped with larger concentrations of Er^{3+} (up to 4 wt%). Optical performance of these doped phosphate glasses suggesting the suitability of these glasses for optical fibre/waveguide amplifiers.
© 2008 Elsevier B.V. All rights reserved.

1. Introduction

Incoherent broadband optical sources, particularly in telecommunication window, are widely used in variety of applications which includes fiber-optic gyroscopes and optoelectronic light source for wavelength division multiplexing systems. Though rare-earth doped, individual or co-doped, glass fibers/waveguides are of great promise, the focus has been concentrated mostly on silicate glasses although their amplified spontaneous emission (ASE) bandwidths are limited to few tens of nanometers (∼40 nm). Quite recently, rare-earth co-doped fluoride and tellurite glasses have shown ASE with considerably extended bandwidths [1–5].

In general, application and utilities of glassy materials are enormous and are governed by the factors like composition, refractive index and dopants/impurities present in the glasses. Moreover, the rare-earth emission in glassy matrix is strongly dependent on crystal field effects, local environment of the rare-earth ion, phonon energies, refractive index and precise details about glass defects (Urbach tails) extended into the band gap. Silicate glasses, mostly being inexpensive, are preferred as host matrix but they have disadvantages such as low refractive index and less rare-earth solubility. Among the other glass hosts, phosphate glasses have been found to be most suitable host for larger rare-earth doping. Significant effects have been made in the recent past in the direction of waveguide and fiber phosphate glass optical amplifier devices [6–8]. However, current available information on phosphate matrix are still incomplete due to unusual structural characteristics such as high co-ordinations of the elements present and the

large number of chemical elements that are being used in the compositions of these glasses. Our recent extensive studies on phosphate glasses reveal the potentiality of these glasses as broadband sources because of their wide region of transparency, moisture and thermal durability and the ability to accept higher percentage of the rare-earths as dopants [9–12].

The present paper deals with the absorption and emission properties of Erbium doped Alkali chlorophosphate glass systems. Absorption spectral intensities of Er^{3+} transitions in various glass compositions are analyzed by Judd–Ofelt theory. The results are examined with respect to composition and the Er^{3+} ion concentration effects, and a comparison has been made with respect to other reported glass systems.

2. Experimental

The glass compositions of xNa$_2$O–$(60 - x)$ PbCl$_2$–40P$_2$O$_5$ ($x = 0, 10, 20$ and 30) (NPPx) were prepared in batches of 10 g. Stoichiometric amounts of $(NH_4)_2HPO_4$, PbCl$_2$ and NaNO$_3$ (Analytical grade) (Aldrich Chemical Co., USA) and were taken in a mortar and were mixed and ground thoroughly using spectroscopic grade iso-proponal. Then the mixture was taken into a silica/porcelain crucible and is placed into a furnace. The temperature was raised slowly to 300 °C and was maintained for about an hour and then slowly increased up to 600 °C, to ensure a complete decomposition of $(NH_4)_2HPO_4$ into P$_2$O$_5$. Subsequently the temperature of the mixture was raised to 900 °C to get a clear melt. The homogeneity of the product was ensured by repeated stirring of the melt. The bubble free and homogeneous melt was poured on a preheated (around 250 °C) brass mould and allowed to cool slowly. Good transparent bulk glasses of dimensions 1 cm × 2 cm × 0.2 cm were obtained by this process, and all the glasses were annealed at 200 °C for 24 h. The glass samples were polished to the commercial quality using a water free lubricant.

Various glass compositions with 1 wt% of Er^{3+} dopant using ErCl$_3$ were prepared for all glass compositions, mentioned above. Glasses with varying Er^{3+} concentration (0.5–4 wt%) for one of the glass composition, NPP20 were also fabricated, to examine the effect of concentration. However, for more than 4 wt% Er^{3+} doping, the glass transparency was lost. Similarly when Na$_2$O content was increased beyond 40, the glass became opaque and moisture sensitive. All the glasses under the study are well-exposed to moisture for long duration and found to be moisture insensitive and weathering durability.

The absorption spectra were recorded on a Perkin–Elmer UV–VIS spectrophotometer. A 488 nm wavelength of Ar-ion laser was used as excitation source to record emission characteristics. The excitation power density was 0.5 W/cm^2. To measure emission and its decay curves, a cooled InGaAs detector, monochromator, mechanical chopper (12 Hz), lock-in amplifier, current amplifier and

digital storage oscilloscope were employed. Refractive index measurements for undoped glasses were carried out by Brewster angle setup consisting of He–Ne laser and a detector.

3. Theory

The molar refractivity (R_m) was calculated by [13]

$$R_m = \frac{\eta^2 - 1}{\eta^2 + 2}\left(\frac{M}{\rho}\right) = \frac{4\pi\alpha_m N_A}{3} \tag{1}$$

where η is the refractive index, M is the molecular weight, ρ is the density, N_A is Avogadro's number and α_m is the polarizability of the molecule. Molar volume (V_m) and dielectric constant (ε) were obtained using the relations $V_m = M/\rho$ and $\varepsilon = \eta^2$, respectively.

The optical band gap (E_{opt}) and Urbach Energies were calculated from absorption spectra of undoped glasses, using the relations discussed elsewhere [9]. The experimental oscillator strengths of various absorption spectral transitions of Er^{3+} doped glasses were obtained from [14,15]

$$f_{exp} = \frac{2303mc^2}{N_A\pi e^2}\int\varepsilon(\bar{v})d\bar{v} \tag{2}$$

where m and e are the electron mass (in g) and charge (in e.s.u.), respectively, c is the velocity of light and $\varepsilon(\bar{v})$, the extinction coefficient, given by $\varepsilon(\bar{v}) = (1/C\ell)\log(I_0/I)$ where C is concentration of Er^{3+} (in moles/litre), ℓ is the optical path length (in cm) and $\log(I_0/I)$ is the absorptivity.

The oscillator strengths for the transitions were also obtained from Judd–Ofelt theory, as

$$f_{cal} = \sigma\sum T_\lambda\langle f^N\psi J|U^\lambda|f^N\psi'J'\rangle^2 \tag{3}$$

where σ is the mean energy of the transition in cm^{-1} and T_λ are the adjustable intensity parameters (The matrix elements are composed of U^λ). Since matrix elements of U^λ are insensitive to ion environment, free-ion matrix elements were taken from literature [15,16]. The experimental oscillator strengths were fitted by least square analysis to obtain the intensity parameters T_λ. These parameters subsequently were used to calculate Judd–Ofelt parameters Ω_λ ($\lambda = 2, 4$ and 6) using the expression

$$\Omega_\lambda(cm^2) = \frac{3h}{8\pi^2mc}\frac{9\eta(2J + 1)T_\lambda}{(\eta^2 + 2)^2} \tag{4}$$

where h is Plank's constant, η is refractive index of the medium and $(2J + 1)$ is the degeneracy of the ground level of the particular ion of interest.

4. Results and discussion

The physical and optical parameters such as refractive index (η), density (ρ), molar refractive index (R_m), molar volume (V_m), optical band gap (E_{opt}) and Urbach energies (ΔE) for the glasses with various Na$_2$O content (at the expense of PbCl$_2$), determined from the experimental data,

are shown in Table 1. The refractive index values show the general trend of decreasing values with the decrease of lead content, except for the glass composition, $x = 10$. In general, all glasses are optically transparent above 320 nm wavelength and optical band gap (E_g) values are estimated from the undoped glass absorption spectra. These E_g values are ranging between 3.50 and 3.70 eV, which are much lower than those values reported for other lead based phosphate glasses [12]. Earlier observations suggest that the introduction of Pb^{2+} ions (as oxide) to the phosphate network creates two non-bridging oxygens (NBOs), while the Na^+ creates single NBOs [17,18]. Similarly, it is also observed that increase of Na_2O content considerably shifts the absorption edge to the shorter wavelengths, predominantly due to the creation of less number of NBOs. Contrary to those observations, present lead bearing glasses (of mixed oxide–halide system) show much less optical band gap values and a decreasing trend with the increase in Na_2O content. This could possibly be due to the influence of double bonded oxygens (DBOs) associated to phosphate network, rather than NBOs [12]. On the other hand, the widths of localized states within the optical band gap

(Urbach energies (ΔE) were also estimated from the absorption spectra of undoped glasses. In the present work these values range between 0.14 and 0.22 eV, which are much closer to those values reported for other phosphate glasses [9–12]. Such lower values suggest minimum defects, leading to long-range order in the present glass systems.

Spectral intensities of different energy transitions for 1 wt% Er^{3+} doped chlorophosphate glasses are analyzed using Eqs. (2–4). The observed and calculated oscillator strengths for various transitions to the ground state $^4I_{15/2}$ of Er^{3+} ions in this glassy matrix are given in Table 2. Lower RMS values suggest a good agreement between experimental and calculated oscillator strengths. It is also observed that the Er^{3+} transitions lower than 350 nm are not observed in these glass systems, due to the cut-off region of absorption (Fig. 1). In general, the oscillator strengths and positions are sensitive to the environment of the rare-earth sites which are occupied in the glass network [14]. These oscillator strengths are subsequently used to evaluate important intensity parameters (Ω_λ ($\lambda = 2, 4$ and 6)), known as Judd–Ofelt parameters, using Eqs. (2) and (3). In general, the Ω_2 values for the Ln^{3+} ions in glasses are intermediate between crystalline oxides and chelating ligands [19,20]. Earlier observations suggest that both covalency and site selectivity of rare-earths with non-centrosymmetric potential contributes significantly to Ω_2 [21]. The other values Ω_4 and Ω_6 are dependent on bulk properties such as viscosity and dielectric constant of the media.

On the other hand, hypersensitive nature of rare-earth ion transitions is a characteristic feature, which is strongly dependent on covalency and site asymmetry. Fig. 2A shows the plot between the oscillator strengths of Er^{3+} intense transitions of both hypersensitive as well as non-hypersensitive, versus the sum of Judd–Ofelt parameters $\sum \Omega_\lambda$ ($\lambda = 2, 4$ and 6). As seen from Fig. 2A, the hypersensitive transitions, $^4I_{15/2} \rightarrow {}^2H_{11/2}$, and $^4I_{15/2} \rightarrow {}^4G_{11/2}$ show relatively higher oscillator strengths compared to non-hypersensitive transitions $^4I_{15/2} \rightarrow {}^4F_{9/2}$ and $^4I_{15/2} \rightarrow {}^4S_{3/2}$, and they are intermediate between ionic and highly

Table 1
Physical and optical properties of xNa_2O–$(60 - x)$ $PbCl_2$–$40P_2O_5$ glasses

Physical/optical property	NPP0	NPP10	NPP20	NPP30
E_{opt} (eV)	3.55	3.57	3.50	3.70
Urbach energy, ΔE (eV)	0.14	0.22	0.18	0.17
Refractive index, η	1.73	1.57	1.64	1.59
Density, ρ (g/cm^3)	5.67	5.17	4.68	3.90
Molecular weight, M (g/mol)	223.64	202.02	180.41	158.8
Molar volume, V_m (cm^3/mol)	39.44	39.08	38.55	40.72
Molar refraction, R_m (cm^3/mol)	15.76	12.78	13.87	13.65
Polarizability, α (A^3)	6.25	5.07	5.50	5.42
Judd–Ofelt parameters and PL life times of 1 wt% Er^{3+} doped glasses				
$\Omega_2 \times 10^{-20}$ (cm^2)	3.36	4.11	3.66	3.79
$\Omega_4 \times 10^{-20}$ (cm^2)	0.51	0.47	0.34	0.13
$\Omega_6 \times 10^{-20}$ (cm^2)	1.51	1.16	1.86	1.21
PL life times, τ (ms)	2.3	2.1	2.4	2.5

$x = 0, 10, 20$ and 30 (denoted as NPP0, NPP10 NPP20 and NPP30, respectively).

Table 2
Experimental and theoretical oscillator strengths of the spectral transitions of 1 wt% Er^{3+} in NPPx glasses

| Transition to	Energy (cm^{-1})	NPP0		NPP10		NPP20		NPP30	
From $^4I_{15/2}$		$f_{obs} \times 10^{-6}$	$f_{cal} \times 10^{-6}$	$f_{obs} \times 10^{-6}$	$f_{cal} \times 10^{-6}$	$f_{obs} \times 10^{-6}$	$f_{cal} \times 10^{-6}$	$f_{obs} \times 10^{-6}$	$f_{cal} \times 10^{-6}$
$^4I_{13/2}$	6447	1.55	1.65	1.48	1.49	1.45	1.80	1.40	1.11
$^4I_{11/2}$	10065	0.65	0.76	0.52	0.71	0.57	0.85	0.54	0.57
$^4I_{9/2}$	12446	0.26	0.14	0.25	0.12	0.18	0.09	0.20	0.42
$^4F_{9/2}$	15298	1.52	1.62	1.25	1.44	1.33	1.61	0.88	0.93
$^4S_{3/2}$	18229	0.62	0.66	0.62	0.62	0.66	0.76	0.40	0.47
$^2H_{11/2}$	19065	5.77	5.70	5.63	5.97	5.53	5.62	4.95	5.30
$^4F_{7/2}$	20339	2.50	2.26	2.57	2.08	3.31	2.49	1.56	1.54
$^4F_{5/2}$	22009	0.88	0.80	0.50	0.75	0.62	0.92	0.43	0.57
$^4F_{3/2}$	22388	0.48	0.46	0.14	0.43	0.29	0.53	0.28	0.33
$^2G_{9/2}$ ($^4F,^2H)_{9/2}$	24371	0.75	0.93	0.49	0.86	0.77	1.04	0.48	0.65
$^4G_{11/2}$	26182	10.00	10.04	10.7	10.6	10.00	9.94	9.60	9.41
RMS ($\times 10^{-6}$)		0.12		0.27		0.33		0.17	

$x = 0, 10, 20$ and 30.
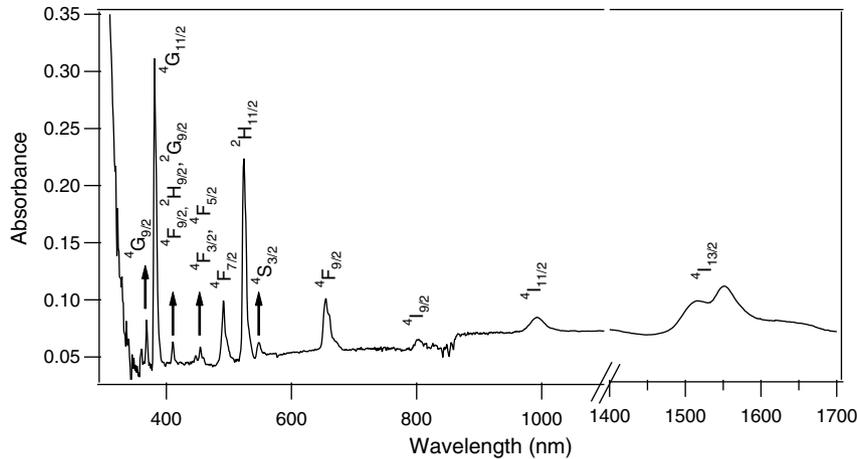
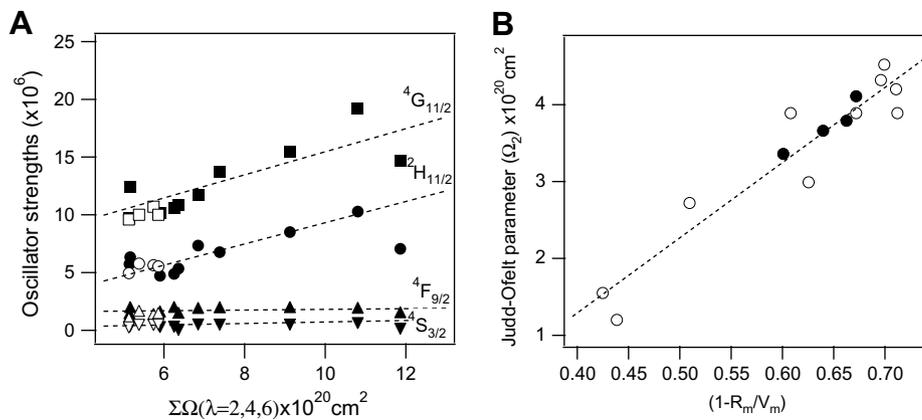Fig. 1. Absorption spectra of 1 wt% Er^{3+} doped NPP10 glass, along with energy transitions from $^4I_{15/2}$.

Fig. 2. (A) Oscillator strengths (as open symbols) of various hypersensitive ($^4G_{11/2}$ and $^2H_{11/2}$) and non-hypersensitive ($^4F_{9/2}$ and $^4S_{3/2}$) transitions of Er^{3+} ions with respect to the sum of Judd–Ofelt parameters, $\sum\Omega_\lambda$ ($\lambda = 2$, 4 and 6). Various other glasses are also incorporated (as filled symbols) for comparison [9,21]. Dashed lines are guide to the eye and (B) Judd–Ofelt parameter Vs metallization parameter $(1 - R_m/V_m)$. Filled circles indicate present data points while the open circles are the data taken for various glass systems reported in Refs. [23–28]. Dashed line indicates the trend of the data.

covalent glasses [9,21]. In our present study, the observed Ω_2 values are close to that of the covalent glasses (like phosphates and tellurites) and on the higher side to the values reported for ionic glasses (fluorides and oxyfluorides) [9].

Electronic polarization of materials is widely regarded as one of the most influencing parameter and many physical, linear and nonlinear optical properties of materials are strongly dependent on it. Duffy, Dimitrov and Sakka correlated many independent linear optical entities to the oxide ion polarizability of single component oxides [13,22]. This polarizability approach, predominantly gives the insight into the strong relation between covalent/ionic nature of materials and other optical parameters, such as optical band gap. Recently we have related optical band gaps of various binary, ternary and quaternary oxide glasses to the polarizability (of cation) in terms of $1 - R_m/V_m$, known as covalency parameter or metallization parameter [9,21]. Generally, the covalency parameter ranges from 0.3 to 0.45 for highly polarisable cation containing oxides (such as Pb^{2+} and Nb^{5+}), while for the alka-

line and alkaline-earth (such as Na^+, Li^+) oxides it falls in between 0.5 and 0.70. Although it is quite complex to correlate optical parameters of the present glassy systems with polarizability of oxide ions, due to the presence of halides, it is interesting to see the influence of cation (Na^+ and/or Pb^{2+}–variation) polarizability on other independent parameters. Here, we attempted to correlate the influence of glass matrix properties on the optical properties of the dopant, that is Er^{3+} ion. Since Ω_2 values are known to show dependence on covalent nature of host, we made a plot between Ω_2 values and metallization parameter $(1 - R_m/V_m)$ in Fig. 2B. Other phosphate glasses [23–28] are also included in the plot for comparison. Interestingly, the Ω_2 values for present chlorophosphates are monotonically increasing with the metallization parameter and lie between 0.6 and 0.7, with comparatively high values of Ω_2. Though with respect to metallization parameters they show more of alkali oxide nature, significantly higher Ω_2 indicates strong covalent nature, could possibly be due to the increased role of phosphate linkage, having more

double bonded oxygens (DBOs) coordinated to the rare-earth ions [12].

The near-infrared PL studies of Er^{3+} ions for the transition $^4I_{13/2} \rightarrow {}^4I_{15/2}$ are recorded by exciting with 488 nm line of Ar^+ laser, that is into the absorption level of $^4F_{7/2}$. The PL band typically exhibits asymmetric shape at ~1540 nm having overall features covering 1400–1650 nm region, with FWHM of 40–45 nm. Low intense emission at 980 nm (FWHM $\leqslant$ 30 nm) (not shown here) of $^4I_{11/2} \rightarrow {}^4I_{15/2}$ transition, with the relative intensity of ~10^{-3} with respect to 1540 nm transition, has also been observed. To observe any concentration influence on PL behavior, the PL measurements for the glass NPP20 doped with varied Er^{3+} ion concentrations (from 0.5 to 4 wt%) were also performed (Fig. 3). Though no peak shift has been observed, the broadness of the emission spectra did show considerably increasing trend (FWHM 43–62 nm) with the increase of Er^{3+} ion concentration. These values are close to the values
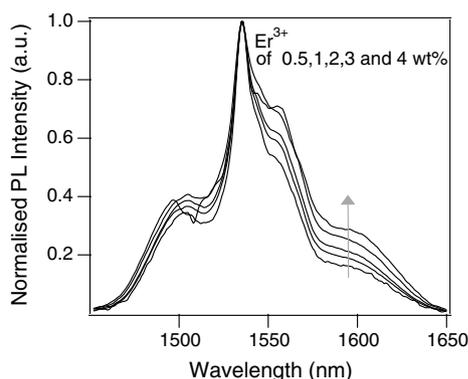
reported for other phosphate glasses [7,26]. The emission broadness with the increase of Er^{3+} concentration could be due to occupation of active ions in various sites of microscopic environment, results into more inhomogeneous broadening. However, observed broadness can also arise from self-absorption and radiation trapping processes [33]. To support such arguments, more experiments such as temperature and length-dependent emission are needed.

The PL decay behavior of $^4I_{13/2} \rightarrow {}^4I_{15/2}$ transition for various glass compositions (with 1 wt% Er^{3+}) are shown in Fig. 4A. All the normalized experimental data, with respect to pump energy, are fitted with the function $y(t) = A \exp(-t/\tau)^{\beta}$, where the adjustable parameter β is found to be very close to 1 (ranging between 0.97 and 0.99) and τ is the emission life time. All the decay curves in the present case convincingly follow a single exponential stretch and the PL life times obtained from the fittings are given in the Table 1. Since the decay function is purely an exponential, the life times (τ) are same as 1/e decay times. These values show a moderate increase with the increase of Na_2O content, except for NPP10, and are generally lower compared to the values reported for other alkaline-free phosphate glasses [29,30].

To design an optical media for short optical amplifiers, it is essential to study the concentration quenching phenomena of rare-earth ion emission [29–31]. Concentration dependent emission quenching is mostly due to the non-radiative transfer of energy to closely neighboring non-excited rare-earth ions, up-conversion and non-radiative relaxation [31,32]. To demonstrate the effect of Er^{3+} ion concentration on PL decay, we have attempted experiments on one of the glasses, NPP20 (Fig 4B). Er^{3+} ion concentrations 0.5, 1, 2, 3 and 4 wt%, were selected as doping in NPP20 and the estimated lifetime values from the PL decay are 3.8, 2.4, 3.2, 2.1 and 1.9 ms ($\pm$0.2 ms), respectively. Compared to the other alkaline-free phosphate

Fig. 3. Photoluminescence spectra ($^4I_{13/2} \rightarrow {}^4I_{15/2}$ transition) of various Er^{3+} concentrations in NPP20 glass. Arrow indicates the increase of concentration
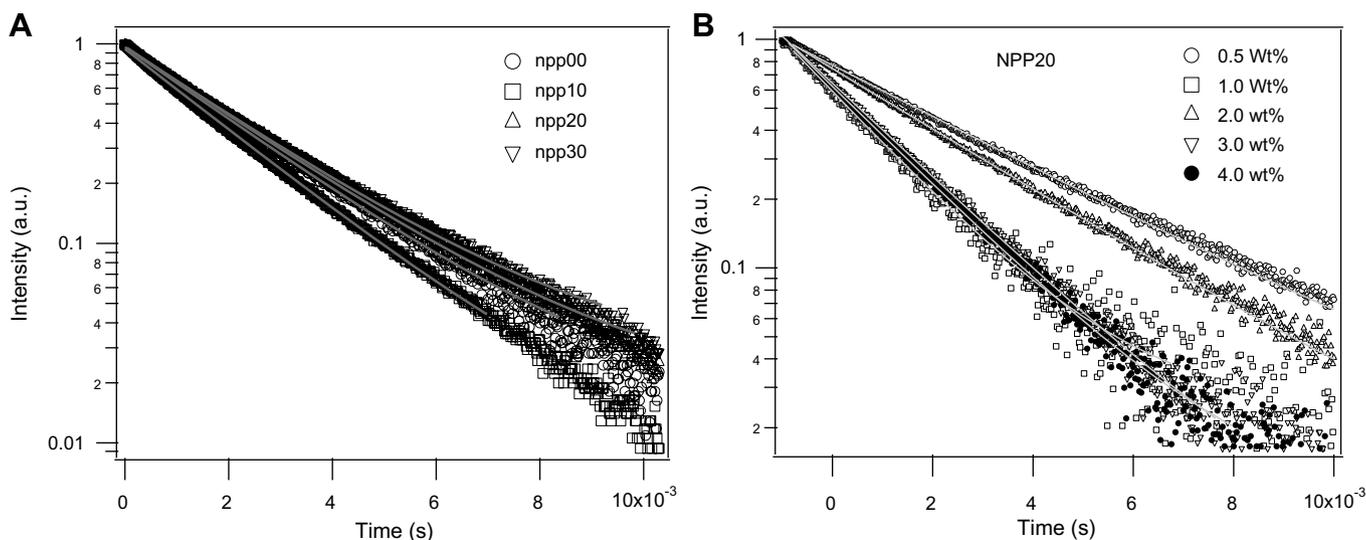

Fig. 4. (A) Photoluminescence decay of 1 wt% Er^{3+} doping in various compositions of NPPx glasses ($x = 0$, 10, 20 and 30) and (B) Photoluminescence decay of various Er^{3+} concentrations (from 0.5 to 4 wt%) in NPP20 glass.

glasses, present glassy systems show intermediate values and are close to the lead containing germinate glasses [29,30]. Though the trends of concentration effect on life times are close to those reported for other phosphate glass [30], present experiential values are very limited for a quantitative conclusion on quenching effects. We have also exposed these alkali chlorophosphate glasses to molten salts of silver and potassium salts at 300–350 °C temperatures to verify the ion-exchange waveguide fabrication compatibility. Experiments are under progress and the preliminary results are suggesting the suitability of these glasses for such applications.

5. Conclusions

In conclusion, we have fabricated a new class of Erbium doped glasses with compositions $x\mathrm{Na_2O}$–$(60 - x)$ $\mathrm{PbCl_2}$–$40\mathrm{P_2O_5}$ ($x = 0$, 10, 20 and 30). In general, all the glasses under study exhibit water resistant and weathering durability. The absorption spectra are analyzed for Judd–Ofelt parameters from the integrated intensities of various absorption bands. We have correlated hypersensitive nature of $\mathrm{Er^{3+}}$ absorption transitions and metallization parameter of glass with Judd–Ofelt parameters to understand the effect of the glass network covalent nature. The photoluminescence and its decay behavior studies are made for all the doped glasses. The Photoluminescence broadness and life times of $^4I_{13/2} \rightarrow {}^4I_{15/2}$ transition were typically in the range of 40–60 nm and 2.13–2.5 ms, respectively and show dependence on the glass composition and rare-earth ion concentration. By and large, these glass systems are capable of taking larger concentration of Erbium and showing their durability for optical applications. These results therefore, suggest that the present alkali phosphate glass systems could be suitable hosts for the optical amplifiers with an intake of more rare-earth ion concentrations than other phosphate glass systems.

References

[1] Optical technologies in motion, European commission's Information society technologies (IST-OPTIMIST), Fifth framework (FP-5, 1998–2002) projects, <www.ist-optimist.org>.

[2] M. Yamada, M. Shimizu, et al., Nippon telegraph and telephone corporation (NTT) technical review 1 (3) (2003) 80;
S. Aozasa et al., Nippon Telegraph and telephone corporation (NTT) technical review 2 (12) (2004) 44, <www.ntt.co.jp>.

[3] Jefferson L. Wagener, Craig W. Hodgson, Michel J.F. Digonnet, Herbert J. Shaw, J. Lightwave Technol. 15 (1997) 1681.

[4] X. Meng, J. Qiu, M. Peng, D. Chen, Q. Zhao, X. Jiang, C. Zhu, Opt. Express 13 (2005) 1628.

[5] L. Huang, A. Jha, S. Shen, X. Liu, Opt. Express 12 (2004) 2429.

[6] R.A. Martin, J.C. Knight, IEEE Photon. Technol. Lett. 18 (2006) 574.

[7] S.F. Wong, E.Y.B. Pun, IEEE Photon. Technol. Lett. 14 (2002) 80.

[8] K. Liu, E.Y.B. Pun, Appl. Opt. 43 (2004) 3179.

[9] G. Vijaya. Prakash, Mater. Lett. 46 (2000) 15, and references therein.

[10] C.R. Mariappan, G. Govindaraj, S.V. Rathan, G. Vijaya Prakash, Mater. Sci. Eng. B 123 (2005) 63.

[11] C.R. Mariappan, G. Govindaraj, S.V. Rathan, G. Vijaya Prakash, Mater. Sci. Eng. B 121 (2005) 2.

[12] G. Vijaya Prakash, R. Jagannathan, Spectrochim. Acta Part A 55 (1999) 1799, and references therein.

[13] V. Dimitrov, S. Sakka, J. Appl. Phys. 79 (1996) 1736.

[14] R. Reisfeld, C.K. Jorgensen, Lasers and Excited States of Rare-earths, Springer Verlag, NY, 1975.

[15] R.D. Peacock, The Intensities of Lanthanide f–f Transitions Structure and Bonding, vol. 22, Springer-Verlag, NY, 1975, 83.

[16] W.T. Carnall, P.R. Fields, K. Rajnak, J. Chem. Phys. 49 (1968) 4424.

[17] K. Subrahmanyam, M. Salagram, Opt. Mater. 15 (2000) 181.

[18] P. Gray, J. Non-Cryst. Solids 68 (1984) 75.

[19] F. Kirby, R.A. Palmer, Inorg. Chem. 20 (1981) 4219.

[20] F. Kirby, R.A. Palmer, Inorg. Chem. 20 (1981) 1030.

[21] P. Nachimuthu, R. Jagannathan, J. Am. Ceram. Soc. 82 (1999) 387.

[22] J.A. Duffy, J. Solid State Chem. 62 (1986) 145.

[23] P. Capek, M. Mika, J. Oswald, P. Tresnakova, L. Salavcova, O. Kolek, J. Schrofel, J. Spirkova, Opt. Mater. 27 (2004) 331.

[24] L.R.P. Kassab, L.C. Courrol, R. Seragioli, N.U. Wetter, S.H. Tatumi, L. Gomes, J. Non-Cryst. Solids 348 (2004) 94.

[25] G.C. Righini, S. Pelli, M. Brenci, M. Ferrari, C. Duverger, M. Montagna, R. Dall'Igna, J. Non-Cryst. Solids 284 (2001) 223.

[26] G.C. Righini, S. Pelli, M. Fossi, M. Brenci, A.A. Lipovskii, E.V. Kolobkova, A. Speghini, M. Bettinelli, Proc. SPIE 4282 (2001) 210.

[27] A.M. Jurdyc, V.G. Truong, B. Jacquier, V. Nazabal, J. Leperson, J.L. Adam, International Workshop on Photonics and Applications, Hanoi, Vietnam, 2004, p. 201, April 5–8.

[28] Y.K. Sharma, S.S.L. Surana, R.K. Singh, R.P. Dubedi, Opt. Mater. 29 (2007) 598.

[29] H. Yamauchi, Y. Ohishi, Opt. Mater. 27 (2005) 679.

[30] H. Desirena, E. De la Rosa, L.A. Diaz-Torres, G.A. Kumar, Opt. Mater. 28 (2006) 560.

[31] J.H. Campbell, T.I. Suratwala, J. Non-Cryst. Solids 263–264 (2000) 318.

[32] C. Jacinto, S.L. Oliveria, L.A.O. Nunes, J.D. Myers, M.J. Myers, T. Catunda, Phys. Rev. B 73 (2006) 125107.

[33] G.C. Righini, M. Ferrari, La Riv. Nuovo Cim. 28 (2005) 1.